研究成果の刊行に関する一覧

【全体研究：糖尿病性腎症症例のレジストリーの作成】

1) Kubo A, Kim YH, Iwano M, et al. The homeobox gene Hex regulates hepatocyte differentiation from embryonic stem cell- derived endoderm. Hepatology 51:633-641, 2010
2) Nakatani K, Yoshimoto S, Iwano M, et al. Fractalkine expression and CD16+ monocytes accumulation in glomerular lesions: Association with their severity and diversity in lupus models. Am J Physiol Renal 299:F207-216, 2010
3) Harada K, Akai Y, Iwano M, et al. Resolution of mesangial light chain deposits three years after high-dose melphalan with autologous peripheral blood stem cell transplantation. Clin Nephrol 74:384-388, 2010
4) Iwano M. EMT and TGF-beta in renal fibrosis. Front Biosci (Schol Ed) 2:229-238 2010
5) 山口通雅、岩野正之、斎藤能彦： 尿中ポドサイト 日本臨床 68 巻 増刊号 9, p441-444
6) 横山仁，田口尚，杉山斉：腎臓病総合レジストリーの構築と応用．日透医雑誌 25（3）：1467-472，2010
7) Saito A, Matsumoto Y, Oyama Y, Asaka M, Yokoyama H. Effectiveness of weekly percutaneous maxacalcitol injection therapy in patients with secondary hyperparathyroidism. Ther Apher Dial, 14:98-103, 2010
8) Ishikawa I, Hayama S, Morita K, Nakazawa T, Yokoyama H, Honda R, Satoh K, Kakuma T. Long-term natural history of acquired cystic disease of the kidney, Ther Apher Dial, 14:409-416, 2010
9) 足立浩樹，木村庄吾，渥美浩克，井村淳子，山谷秀喜，浅香充宏，友杉直久，横山 仁：慢性移植腎障害に対する脂質およびアディポネクチンの検討，Therapeutic Research, 31：29-31，2010
10) Atsumi H, Asaka M, Kimura S, Imura J, Fujimoto K, Chikazawa Y, Nakagawa M, Okuyama H, Yamaya H, Moriyama M, Tanaka T, Suzuki K, Yokoyama H. A case of second renal transplantation with acute antibody-mediated rejection complicated with BK virus nephropathy. Clin. Transplant 24:35-38, 2010
11) 中川 卓，木村庄吾，藤本圭司，渥美浩克，井村淳子，近澤芳寛，奥山 宏，山谷秀喜，浅香充宏，横山 仁：腹水を伴う肝硬変合併腎不全に腹膜透析を導入した 2 例-日本における報告例のまとめ-，日透析医学会誌，43：93-98，2010
12) 山谷秀喜，横山 仁：糸球体疾患に伴う ARF・AKI，日腎会誌，52：548-552，2010.

【分科会：糖尿病性腎症の病気分類ならびに病態の解析】

1) 草野英二，西野克彦：平成 21 年度 生活習慣病等調査研究事業・慢性腎臓病疾患に関する実態調査(One Day)調査，2010
2) Shikata K, Haneda M, Koya D, Suzuki Y, Tomino Y, Yamada K, Maeda S, Kawakami

N, Uzu T, Nishimura M, Sato C, Ogawa D, Makino H; DNETT-Japan Study Group. Diabetic Nephropathy Remission and Regression Team Trial in Japan (DNETT-Japan): Rationale and study design. Diabetes Res Clin Pract 87, 228-232, 2010

3) Ogawa D, Kahara K, Shigematsu T, Fujii S, Hayakawa N, Okazaki M, Makino H. Optimal cutoff point of waist circumference for the diagnosis of metabolic syndrome in Japanese subjects. J Diabetes Invest 1, 117-120, 2010

4) 小川大輔, 槇野博史：糖尿病腎症のエビデンス, 糖尿病ナビゲーター（第2版）, 300-301, 2010

5) Yamagata K, Makino H, Akizawa T, Iseki K, Itoh S, Kimura K, Koya D, Narita I, Mitarai T, Miyazaki M, Tsubakihara Y, Watanabe T, Wada T, Sakai O, and Advisory Committee for FROM-J. Design and methods of a strategic outcome study for chronic kidney disease - Frontier of Renal Outcome Modifications in Japan (FROM-J) –Clin Exp Nephrol 14; 144-151, 2010

6) Iseki K. Renal outcomes in chronic kidney disease. Nephrology 15: S273-S276, 2010

7) Iseki K, Chiho Iseki, and Kozen Kinjo.C-reactive protein is a predictor for developing proteinuria in a screened cohort. Nephron Clin Pract 117: C51-C56, 2011

8) Jardine MJ, Ninomiya T, Perkovic V, Cass A, Turnbull F, Gallagher MP, Zoungas S, Heerspink HJL, Chalmers J, Zanchetti A. Aspirin is beneficial in hypertensive patients with chronic kidney disease a post-hoc subgroup analysis of a randomized controlled trial. J Am Coll Cardiol 56: 956-65, 2010

9) Heerspink HJL, Ninomiya T, Perkovic V, Woodward M, Zoungas S, Cass A, Cooper M, Grobbee DE, Mancia G, Mogensen CE, Neal B, Chalmers J; for the ADVANCE Collaborative Group. Effects of a fixed combination of perindopril and indapamide in patients with type 2 diabetes and chronic kidney disease. Eur Heart J 31: 2888-96, 2010

10) Ninomiya T, Zoungas S, Neal B, Woodward M, Patel A, Perkovic V, Cass A, Cooper M, Grobbee D, Hamet P, Harrap S, Liu L, Mancia G, Mogensen CE, Poulter N, Rodgers A, Williams B, MacMahon S, Chalmers J; ADVANCE Collaborative Group. Efficacy and safety of routine blood pressure lowering in older patients with diabetes: results from the ADVANCE trial. J Hypertens 28: 1141-9, 2010

11) Nagata M, Ninomiya T, Doi Y, Yonemoto K, Kubo M, Hata J, Tsuruya K, Iida M, Kiyohara Y. Trends in the prevalence of chronic kidney disease and its risk factors in a general Japanese population: the Hisayama Study. Nephrol Dial Transplant 25: 2557-64, 2010

12) Bouchi R, et al. Relationship between chronic kidneydisease and silent cerebral infarction in patients with type 2 diabetes. Diabet Med 27: 538-543, 2010

13) Bouchi R, et al. Silent cerebral infarction is associated with the development and progression ofnephropathy in patients with type 2 diabetes. Hypertens Res 33: 1000-1003, 2010

【分科会：糖尿病性腎症の評価のためのバイオマーカー開発】

1) Mizutani M, Ito Y, Mizuno M, Nishimura H, Suzuki Y, Hattori R, Matsukawa Y, Imai M, Oliver N, Goldschmeding R, Aten J, Krediet RT, Yuzawa Y, Matsuo S. Connective tissue growth factor(CTGF/CCN2) is increased in peritoneal dialysis patients with high peritoneal solute transport rate. Am J Physiol Renal Physiol. 298 (3): F721-33. 2010
2) Ito Y, Goldschmeding R, Kasuga H, Claessen N, Nakayama M, Yuzawa Y, Sawai A, Matsuo S, Weening JJ, Aten J. Expression patterns of connective tissue growth factor and of TGF{beta} isoforms during glomerular injury recapitulate glomerulogenesis. Am J Physiol Renal Physiol. 299(3): F545–F558, 2010
3) Sawai A, Ito Y, Mizuno M, Suzuki Y, Toda S, Ito I, Hattori R, Matsukawa Y, Gotoh M, Takei Y, Yuzawa Y, Matsuo S., Peritoneal macrophage infiltration is correlated with baseline peritoneal solute transport rate in peritoneal dialysis patients. Nephrol Dial Transplant. 2010 Nov 22. , Epub ahead of print
4) Misu H, Takamura T, Takayama H, Hayashi H, Matsuzawa-Nagata N, Kurita S, Ishikura K, Ando H, Takeshita Y, Ota T, Sakurai M, Yamashita T, Mizukoshi E, Honda M, Miyamoto K, Kubota T, Kubota N, Kadowaki T, Kim HJ, Lee IK, Minokoshi Y, Saito Y, Takahashi K, Yamada Y, Takakura N, Kaneko S: A liver-derived secretory protein, selenoprotein p, causes insulin resistance. Cell Metab 12:483-495, 2010
5) Hamaguchi E, Takamura T, Sakurai M, Mizukoshi E, Zen Y, Takeshita Y, Kurita S, Arai K, Yamashita T, Sasaki M, Nakanuma Y, Kaneko S: Histological course of nonalcoholic fatty liver disease in Japanese patients: tight glycemic control, rather than weight reduction, ameliorates liver fibrosis. Diabetes Care 33:284-286, 2010
6) Ootsuji H, Honda M, Kaneko S, Usui S, Okajima M, Okada H, Sakai Y, Takamura T, Horimoto K, Takamura M: Altered hepatic gene expression profiles associated with myocardial ischemia. Circ Cardiovasc Genet 3:68-77, 2010
7) Ando H, Ushijima K, Kumazaki M, Eto T, Takamura T, Irie S, Kaneko S, Fujimura A: Associations of metabolic parameters and ethanol consumption with messenger RNA expression of clock genes in healthy men. Chronobiol Int 27:194-203, 2010
8) Ando H, Ushijima K, Kumazaki M, Takamura T, Yokota N, Saito T, Irie S, Kaneko S, Fujimura A: Influence of age on clock gene expression in peripheral blood cells of healthy women. J Gerontol A Biol Sci Med Sci 65:9-13, 2010
9) Kobayashi D, Takamura M, Murai H, Usui S, Ikeda T, Inomata JI, Takashima SI,

Kato T, Furusho H, Takeshita Y, Ota T, Takamura T, Kaneko S: Effect of pioglitazone on muscle sympathetic nerve activity in type 2 diabetes mellitus with alpha-glucosidase inhibitor. Auton Neurosci 158:86-91, 2010
10) Komura T, Sakai Y, Honda M, Takamura T, Matsushima K, Kaneko S: CD14+ monocytes are vulnerable and functionally impaired under endoplasmic reticulum stress in patients with type 2 diabetes. Diabetes 59:634-643, 2010
11) 山本　格：腎臓病のプロテオーム解析, Modern Physician 31(1),190-193,2011
12) 山本　格：腎臓病のプロテオーム解析, 日本内科学会雑誌 99(7), 1671-1677,　2010
13) 山本　格：腎臓病学におけるプロテオミクス, 日本腎臓学会誌 52(4),　457-460,　2010
14) 山本　格：Human Proteome Organization (HUPO)のヒト腎臓・尿プロテオームプロジェクト, 新潟医学会雑誌 124(2), 55-64,2010
15) 山本　格：糸球体タンパク質のデータベース,　病理と臨床 28(5),524-529,2010
16) 山本　格：バイオインフォマティクスの利用法(1),　Nephrology Frontier, 9(3), 297-300, 2010
17) 山本　格：バイオインフォマティクスの利用法(2),　Nephrology Frontier, 9(4), 398-403, 2010

【分科会:糖尿病性腎症の新規治療法の開発】

1) Fujimi-Hayashida A, Ueda S, Yamagishi S, Kaida Y, Ando R, Nakayama Y, Fukami K, Okuda S. Association of asymmetric dimethylarginine with severity of kidney injury and decline in kidney function in IgA nephropathy.Am J Nephrol.33(1):1-6, 2011.
2) Nagano M, Fukami K, Yamagishi SI, Sakai K, Kaida Y, Matsumoto T, Hazama T, Tanaka M, Ueda S, Okuda S. Tissue level of advanced glycation end products (AGEs) is an independent determinant of high sensitive C-reactive protein levels in hemodialysis patients. Nephrology. 2010 Nov 3. doi: 10.1111/j.1440-1797.2010.01419.x.
3) Matsui T, Yamagishi S, Takeuchi M, Ueda S, Fukami K, Okuda S. Nifedipine inhibits advanced glycation end products (AGEs) and their receptor (RAGE) interaction-mediated proximal tubular cell injury via peroxisome proliferator-activated receptor-gamma activation. Biochem Biophys Res Commun. 23;398(2):326-30, 2010.
4) Yoshimura J, Fukami K, Koike K, Nagano M, Matsumoto T, Iwatani R, Kusumoto T, Hazama T, Ueda S, Adachi H, Hirai Y, Takasu K, Ohshima K, Yamagishi S, Okuda S. Interstitial Foxp3-positive T cells may predict renal survival in patients with myeroperoxidase anti-neutrophil cytoplasmic antibody-associated glomerulonephritis. Clin Exp Pharmacol Physiol.37(9):879-83, 2010

5) Fukami K, Yamagishi SI, Okuda S. Development of enzyme-linked immunosorbent assay system for PEDF and its clinical utility. Curr Mol Med. 2010 Apr;10(3):317-20
6) Matsui T, Yamagishi S, Ueda S, Fukami K, Okuda S. Irbesartan inhibits albumin-elicited proximal tubular cell apoptosis and injury in vitro. Protein Pept Lett. 17(1):74-7, 2010
7) Kitada M, Shinji K, Imaizumi N, Koya D: Resveratorol improves oxidative stress through normalization of Mn-SOD dysfunction in AMPK/SIRT1-1-independent pathway, Diabetes, in press
8) Kume S, Uzu T, Horiike K, Chin-Kanasaki M, Isshiki K, Araki S, Sugimoto T, Haneda M, Kashiwagi A, Koya D. Calorie restriction enhances cell adaptation to hypoxia through Sirt1-dependent mitochondrial autophagy in mouse aged kidney. J Clin Invest 120, 1043-1055, 2010
9) Araki S, Haneda M, Koya D, Isshiki K, Kume S, Sugimoto T, Kawai H, Nishio Y, Kashiwagi A, Uzu T, Maegawa H. Association between urinary type IV collagen level and deterioration of renal function in type 2 diabetic patients without overt proteinuria. Diabetes Care, 33, 1805-1810, 2010
10) Soumura M, Kume S, Isshiki K, Takeda N, Araki S, Tanaka Y, Sugimoto T, Chin-Kanasaki M, Nishio Y, Haneda M, Koya D, Kashiwagi A, Maegawa H, Uzu T. Oleate and eicosapentaenoic acid attenuate palmitate-induced inflammation and apoptosis in renal proximal tubular cell. Biochem Biophys Res Commun. 402, 265-271, 2010
11) 古家大祐：糖尿病性腎症, CKD のサイエンス 基礎と臨床 19-30, 2010
12) 古家大祐：糖尿病/耐糖能障害、AKI と CKD のすべて 113-118,2010
13) 古家大祐, 北田宗弘:糖尿病性腎症の発症・進行の原因は?これを阻止する方法はあるか? 糖尿病性腎症でみられる検査異常, 知りたいことがわかる糖尿病性腎症教室 35-46, 59-72, 2010
14) 和田隆志:糖尿病性腎症, 日本腎臓学会会誌, 52, 7,2010
15) Sakai N, Furuichi K, Shinozaki Y, Yamauchi H, Toyama T, Kitajima S, Okumura T, Kokubo S, Kobayashi M, Takasawa K, Takeda S, Yoshimura M, Kaneko S, Wada T. Fibrocytes are involved in the pathogenesis of human chronic kidney disease. Human Pathol 41, 672-678,2010
16) Wada T, Sakai N, Sakai Y, Matsushima K, Kaneko S, Furuichi K. Involvement of bone marrow-derived cells in kidney fibrosis. Clin Exp Nephrol ,in press
17) Kodera R, Shikata K, Kataoka HU, Takatsuka T, Miyamoto S, Sasaki M, Kajitani N, Nishishita S, Sarai K, Hirota D, Sato C, Ogawa D, Makino H. Glucagon-like peptide-1 receptor agonist ameliorates renal injury through its anti-inflammatory action without lowering blood glucose level in a rat model of type 1 diabetes.

Diabetologia.in press

研究成果の刊行物・別刷

The Homeobox Gene *Hex* Regulates Hepatocyte Differentiation from Embryonic Stem Cell–Derived Endoderm

Atsushi Kubo,[1,2] Yon Hui Kim,[3] Stefan Irion,[4] Shogo Kasuda,[5] Mitsuaki Takeuchi,[1,2] Kazuo Ohashi,[6,7] Masayuki Iwano,[1] Yoshiko Dohi,[2] Yoshihiko Saito,[1] Ralph Snodgrass,[3] and Gordon Keller[4]

We investigated the role of the hematopoietically expressed homeobox (*Hex*) in the differentiation and development of hepatocytes within embryonic stem cell (ESC)–derived embryoid bodies (EBs). Analyses of hepatic endoderm derived from $Hex^{-/-}$ EBs revealed a dramatic reduction in the levels of albumin (*Alb*) and alpha-fetoprotein (*Afp*) expression. In contrast, stage-specific forced expression of *Hex* in EBs from wild-type ESCs led to the up-regulation of *Alb* and *Afp* expression and secretion of *Alb* and transferrin. These inductive effects were restricted to c-kit$^+$ endoderm-enriched EB-derived populations, suggesting that *Hex* functions at the level of hepatic specification of endoderm in this model. Microarray analysis revealed that *Hex* regulated the expression of a broad spectrum of hepatocyte-related genes, including fibrinogens, apolipoproteins, and cytochromes. When added to the endoderm-induced EBs, bone morphogenetic protein 4 acted synergistically with Hex in the induction of expression of *Alb*, *Afp*, carbamoyl phosphate synthetase, transcription factor 1, and CCAAT/enhancer binding protein α. These findings indicate that Hex plays a pivotal role during induction of liver development from endoderm in this *in vitro* model and suggest that this strategy may provide important insight into the generation of functional hepatocytes from ESCs. (HEPATOLOGY 2010;51:633-641.)

In the mouse embryo, the liver is first detected as an outgrowth bud of proliferating endodermal cells in the ventral foregut on day 8 of gestation.[1-3] The liver develops in close proximity to the cardiac mesoderm, which produces fibroblast growth factor 1 and 2, which in turn are required for the outgrowth of the ventral foregut endoderm[2,4] and the induction of several liver-specific genes, including albumin (*Alb*) and α-fetoprotein (*Afp*).[5] In addition to fibroblast growth factors, bone morphogenetic protein 4 (BMP-4) expressed in the septum transversum mesenchyme[6] has been shown to be essential for early liver development. In the absence of BMP-4, the foregut endoderm does not thicken, and consequently a distinct liver bud does not form. In spite of the lack of liver bud formation in BMP-4–null embryos, *Alb* expression is induced, suggesting that this factor may play a role in the proper movement of hepatoblasts into the developing liver. Beyond the induction stage, numerous other transcription factors are required for endoderm patterning and organ development. Among these, the hemato-

Abbreviations: Afp, alpha-fetoprotein; Alb, albumin; BMP-4, bone morphogenetic protein 4; Cps1, carbamoyl phosphate synthetase; Dlk1, Delta-like 1; Dox, doxycycline; EB, embryoid body; ECD, E-cadherin; ESC, embryonic stem cell; GAPDH, glyceraldehyde 3-phosphate dehydrogenase; Hex, hematopoietically expressed homeobox; mRNA, messenger RNA; RT-PCR, reverse-transcription polymerase chain reaction; Tcf1, transcription factor 1.

From the [1]First Department of Internal Medicine and the Departments of [2]Public Health, [5]Legal Medicine, and [6]Surgery, Nara Medical University, Nara, Japan; [3]VistaGen Therapeutics, Inc., South San Francisco, CA; the [4]McEwen Center for Regenerative Medicine, University Health Network, Toronto, Ontario, Canada; and the [7]Institute of Advanced Biomedical Engineering and Science, Tokyo Women's Medical University, Tokyo, Japan.

Received March 13, 2009; accepted September 2, 2009.

Supported in part by grants from the Ministry of Education, Sports, Science, and Technology of Japan (17790197) and the Uehara Memorial Foundation (to A. K.) and Special Coordination Funds for Promoting Science and Technology from the Ministry of Education, Sports, Science, and Technology of Japan (to K.O.).

Address reprint requests to: Atsushi Kubo, Nara Medical University, First Department of Internal Medicine, 840 Shijo, Kashihara, Nara, Japan. E-mail: akubo@naramed-u.ac.jp.

Copyright © 2009 by the American Association for the Study of Liver Diseases.

Published online in Wiley InterScience (www.interscience.wiley.com).

DOI 10.1002/hep.23293

Potential conflict of interest: Dr. Snodgrass owns stock in VistaGen Therapeutics.

Additional Supporting Information may be found in the online version of this article.

poietically expressed homeobox gene *Hex* (also known as *Prh*)[7-9] is of particular interest, because it has been shown to play a pivotal role in hepatic development.

Hex is expressed at multiple sites in the developing embryo, including the yolk sac and the region of gut endoderm that gives rise to the liver and thyroid bud.[10-12] Analysis of *Hex*-null embryos demonstrated that formation of the liver bud initiates in the absence of a functional protein and that expression of liver-specific genes including *Alb*, *Afp*, and *Ttr* is up-regulated in this endodermal population.[13,14] Whereas the early stages of morphogenesis to a columnar structure can be detected in these mutant embryos, development beyond day 9.5 of gestation does not proceed and expression of *Alb* is no longer evident,[13-15] suggesting that Hex is required to promote growth and differentiation of the hepatoblast stage of development. Taken together, these studies demonstrate that Hex is essential for the development of liver from gut endoderm and that it functions downstream of the signaling pathways that regulate the specification of the hepatic lineage.

Defining the pathways and transcription factors that regulate lineage commitment in the early embryo is essential for our basic understanding of developmental biology as well as for establishing strategies for the directed lineage-specific differentiation of ESCs in culture. By translating findings from the embryo to this *in vitro* model, it has been possible to develop approaches for the efficient and reproducible induction of endoderm and early hepatic and pancreatic cell fates from both mouse and human ESCs.[16-18] Although the above studies have established the principal signaling pathways regulating hepatic specification, none has investigated the role of the key transcription factors in this process. In the present report, we have used the ES/EB model to study the role of Hex in hepatocyte development *in vitro* and demonstrate that as in the early embryo, this transcription factor is essential for the establishment of hepatocyte lineage.

Materials and Methods

Growth and Differentiation of ESCs. The development and characterization of $Hex^{+/+}$, $Hex^{+/-}$, and $Hex^{-/-}$ ESC lines,[15] the GFP-Bry ESC line,[19] and tet-Hex ESCs[20] have been described. Bry-Ainv cells were generated by targeting green fluorescent protein to the brachyury locus in the Ainv 18 ESC line[19,21] (unpublished data). The Hex-plox targeting plasmid was electroporated into the Bry-Ainv cells, yielding tet-Hex Bry-Ainv ESCs. ESCs were maintained on irradiated mouse embryo fibroblast feeder cells as described.[22]

To assess the function of Hex in developmental progression of hepatocytes during ESC differentiation, tet-Hex ESCs, in which *Hex* expression can be induced by exposure to doxycycline (Dox) at specific time points, were cultured as previously described for ectoderm with some modification.[20] For differentiation of endoderm, activin induction was performed using a two-step protocol as described.[22] To induce Hex expression, Dox (1-30 μg/mL in Iscove's modified Dulbecco's medium with 15% SR and 2 mM glutamine) was added to the cultures at different stages and for varying periods of time. After a total of 10 days of differentiation, EBs were replated on Matrigel-coated 6-well dishes in Iscove's modified Dulbecco's medium supplemented with 15% fetal bovine serum (Vitromex, Geilenkirchen, Germany), 2 mM glutamine, and 10^{-6} M dexamethasone. Cells from these replated cultures were harvested at the indicated times (total differentiation time) for RNA isolation and immunostaining. Alternatively, serum-induced hepatic differentiation was performed as described.[22]

Gene Expression Analysis. For reverse-transcription polymerase chain reaction (RT-PCR), total RNA was extracted using RNeasy mini-kits and then treated with RNase free DNase (Qiagen, Valencia, CA). One microgram of total RNA was then reverse-transcribed to complementary DNA using a Superscript RT kit (Invitrogen, Carlsbad, CA) with random hexamers. PCR was performed using Taq polymerase (Takara Bio, Shiga, Japan) in PCR buffer containing 2.5 mM $MgCl_2$ and 0.2 μM dNTPs. Oligonucleotide primers were performed using the primer pairs shown in Supporting Table 1.

For real-time PCR, commercially available assay mixes for *Alb*, *Afp*, carbamoyl phosphate synthetase (*Cps1*), transcription factor 1 (*Tcf1*), *Hex*, *BMP-4*, Delta-like 1 (*Dlk1*), and glyceraldehyde 3-phosphate dehydrogenase (*GAPDH*) were used to quantify messenger RNA (mRNA) levels, and PCR was performed using a Prism 7700 Sequence Detector (Applied Biosystems, Foster City, CA). mRNA levels were normalized to GAPDH mRNA levels in the same samples.

Fluorescence-Activated Cell Sorting Analysis and Cell Sorting. EBs-derived cells were stained with a PE-conjugated anti-c-kit antibody (BD PharMingen, San Diego, CA), after which the cells were analyzed using a FACSan (Becton Dickenson, San Jose, CA) or sorted on a FACS Aria cell sorter (Becton Dickenson).

Immunostaining. Foxa2 staining of brachyury$^+$ and c-kit$^+$ cells was performed in microtiter wells as described.[22] Briefly, the cells were incubated with an anti-Foxa2 primary antibody (goat polyclonal P-19; Santa Cruz Biotechnololgy, Santa Cruz, CA) and visualized using Cy3-conjugated anti-goat secondary immunoglobu-

lin G antibody (Jackson Immunoresearch, West Grove, PA). For Alb staining, day 14 EBs were scraped, embedded in Tissue Tek O.C.T. compound (Sakura, Torrance, CA), and frozen in liquid nitrogen, after which 4-μm-thick sections were cut on a cryostat and placed on poly-lysine-coated glass microscope slides. After the fixation and permeabilization, the cells were incubated for 1 hour with anti-Alb primary antibody (Biogenesis, Kingston, NH) and visualized using a Cy3-conjugated anti-rabbit immunoglobulin G secondary antibody (Jackson Immunoresearch).

Measurement of Alb and Transferrin Secretion from Day 14 EBs. After culturing EBs for 14 days under various conditions, the medium was changed to serum-free Iscove's modified Dulbecco's medium containing 2 mM glutamine. The EBs were then incubated for an additional 24 hours, and the conditioned medium was collected for assay. Alb and transferrin concentrations in the conditioned medium were measured using solid-phase sandwich enzyme-linked immunosorbent assays (Bethyl, Montgomery, TX) according the manufacturer's instructions.

Microarray Analysis. For microarray analysis, total RNA was extracted using RNeasy mini kits (Qiagen), after which 10 μg of fragmented target total RNA was used for hybridization of each UniSet Mouse I Expression Bioarray chip (Amersham Life Sciences, Buckinghamshire, UK), which contained 10,012 probes. Once the microarrays were hybridized and washed, biotin-containing transcripts were directly detected using a Streptavidin-Alexa647 conjugate. GeneSpring 6.2 (Silicon Genetics, Inc., Redwood City, CA) was then used to evaluate the data obtained using CodeLink Expression Scanning Software.

Target Preparation and CodeLink™ Microarray Analysis. Total RNA was isolated from cell samples using the RNeasy mini kit (Qiagen). One microgram of purified, DNase-treated total RNA was used to synthesize biotinylated cRNA target preparation using the CodeLink™ Expression Assay Reagent Kit (Amersham) according to manufacturer's instructions. Ten micrograms of fragmented cRNA was applied to the Uniset Mouse I Expression Bioarray, hybridized for 18 hours, and the arrays processed according to manufacturer's instructions using Streptavidin-Alexa647 detection reagents. Slides were scanned using a GenePix 4000B scanner (Axon) and the images were analyzed with CodeLink™ Expression Analysis Software.

Results

Hex Regulates Expression of Hepatocyte-Related Genes and Secretion of Their Products. To investigate the role played by Hex in hepatocyte lineage commitment during EB differentiation, we induced endoderm formation from wild-type ($Hex^{+/+}$), heterozygous ($Hex^{+/-}$), or Hex-deficient ($Hex^{-/-}$) ESCs[15] using the serum induction protocol that we have described.[22] Consistent with our earlier findings, the hepatocyte genes *Alb* and *Afp* were both expressed in EBs generated from the $Hex^{+/+}$ and $Hex^{+/-}$ ESCs. The levels of expression of both genes were markedly reduced in the $Hex^{-/-}$ EBs (Fig. 1A). These findings are in line with those from studies on the early embryo, demonstrating that Hex is required for development of the liver *in vivo*.[13,15]

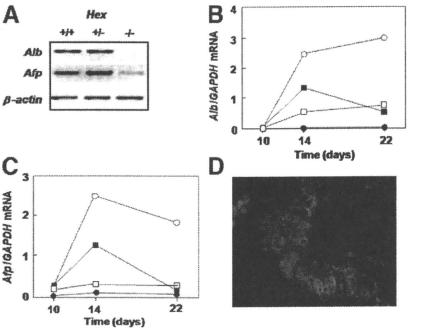

Fig. 1. Hepatocyte differentiation in the presence or absence of *Hex* during endoderm induction. (A) Hepatic differentiation of *Hex*-deficient ESCs. RT-PCR analysis was conducted for EBs generated from $Hex^{+/+}$ (+/+), $Hex^{+/-}$ (+/−), and $Hex^{-/-}$ (−/−) ESCs. Cells were cultured in the serum-induced protocol for hepatocytes for 14 days. (B,C) Time course of *Alb* (B) and *Afp* (C) mRNA expression during hepatic EB differentiation. Differentiation was induced by culture in the following protocols: (1) wild-type ESCs were cultured in serum induction protocol for hepatocytes (□); and (2) tet-Hex ESCs were cultured in the presence of activin for days 2-6 and then cultured without Dox (●) or with Dox on days 6-10 (○) or on days 6-22 (■). *Alb* and *Afp* mRNA levels were quantified by way of real-time PCR and normalized to *GAPDH* mRNA levels. *Alb* and *Afp* mRNA levels are indicated as a ratio compared with those in day 14 fetal liver. (D) Immunostaining of Alb in day 14 EBs cultured with activin with Dox (days 6-10).

To further evaluate the role of Hex in hepatic specification in the ESC/EB model, we used an ESC line (AINV18) that enables the regulated expression of a given gene under the control of a tet-inducible promoter. Using this system, we generated ESCs in which Hex expression was induced by the addition of the tetracycline analogue Dox (tet-Hex ESCs). *Hex* expression was induced in the cells by the addition of Dox (1 μg/mL) to the EB cultures either from days 6-10 or from days 6-22 of differentiation. Quantitative PCR analyses revealed that induction of *Hex* between days 6 and 10 of culture resulted in a significant up-regulation of *Afp* and *Alb* expression com-

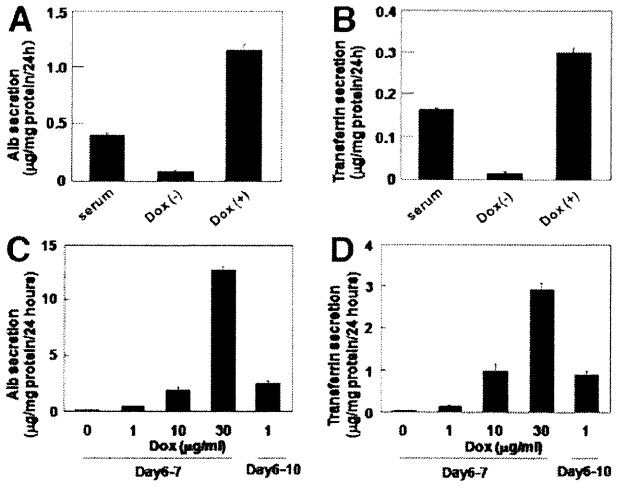

Fig. 2. Secretion of albumin and transferrin from hepatic EBs. (A,B) Differentiation was induced by culture in the following protocols: (1) wild-type ESCs were cultured in the serum induction protocol for hepatocytes (serum); and (2) tet-Hex ESCs were cultured in the presence of activin for days 2-6 and then cultured without Dox (Dox−) or with Dox on days 6-10 (Dox+). At day 14, EBs were cultured in serum-free media for an additional 24 hours. At this point, the media was harvested and the levels of Alb (A) and transferrin (B) were measured using a specific enzyme-linked immunosorbent assay. (C,D) Secretion of Alb (C) and transferrin (D) from activin-induced EBs cultured for 14 days. Cells were treated with Dox at the indicated concentrations for the indicated durations. At day 14, EBs were cultured in serum-free media for an additional 24 hours. At this point, the media was harvested and the levels of Alb and transferrin were measured using specific enzyme-linked immunosorbent assays.

pared with the uninduced cultures (Fig. 1B,C). These levels of expression at day 14 represent 2.6% and 2.5% of the expression found in the fetal liver, respectively. By contrast, when *Hex* was continuously expressed from day 6 to day 22, levels of *Alb* and *Afp* mRNA were diminished on day 22 (Fig. 1B,C), suggesting that prolonged *Hex* expression may disrupt hepatic differentiation or shift the tissue into another fate. Immunostaining showed the presence of clusters of Alb^+ cells within the *Hex*-induced day 14 EBs (Fig. 1D). Hex induction also resulted in enhanced secretion of both Alb and transferrin by the EB-derived cells at day 14 of culture (Fig. 2A,B). These levels of secretion were 7.6% and 5.0% of that of day 14 fetal liver cells, respectively.[23] Taken together, these findings indicate that enforced expression of *Hex* at appropriate stages of differentiation and for a specific period enhances the specification of hepatocyte-like cells from definitive endoderm.

Microarray Analysis of Genes Downstream of Hex. For a more in-depth analysis of the impact of Hex expression on lineage development, we performed a microarray analysis to identify genes activated downstream of Hex. For these studies, we compared the following populations: (1) cells from day 14 hepatocyte cultures to cells from day 6 EB cells that were induced to form mesoderm by a continuous exposure to serum; (2) cells from day 14 $Hex^{+/+}$ hepatoycte cultures to cells from day 14 $Hex^{-/-}$ hepatocyte cultures; and (3) and cells from 14-day hepatocyte cultures derived from Hex-induced EBs to a comparable population derived from noninduced EBs. For the third analyses, endoderm was induced with activin and Hex was induced by the addition of Dox from days 6 to 10 of differentiation.

The findings from these different analyses are summarized in Supporting Table 2. These microarray data are provided online. Of the 10,012 genes analyzed, the outcome of the first comparison revealed that the expression levels of 1,155 were significantly up-regulated in endoderm/hepatocyte conditions, in both mesodermal EBs and undifferentiated ESCs ($P < 0.05$) (comparison). Of these 1,155 genes, 240 were expressed at significantly higher levels ($P < 0.05$) in the day 14 $Hex^{+/+}$ hepatocyte cultures compared with the day 14 $Hex^{-/-}$ hepatocyte cultures (comparison 2). Thirty-four of the 240 genes were also up-regulated following Dox induction (comparison 3, tet-Hex Dox(+)/Dox (−) (Supporting Table 2). The genes shown to be regulated by *Hex* expression could be categorized into five functional groups: (1) serum protein genes such as alb1; (2) coagulation-related genes such as fibrinogens; (3) lipid-related genes such as apolipoproteins; (4) growth factor related genes such as insulin-like growth factor binding protein; and (5) others. The fact that most of these proteins are produced in the liver adds further support to the interpretation that forced expression of Hex at appropriate stages of development efficiently induces liver specification and maturation from the ESC-derived endoderm.

Treatment with a High Concentration of Dox at the Appropriate Time Induces Maturation of Hepatocytes During ESC Differentiation. To define more precisely the time frame during which *Hex* exerts this effect, Dox was added from days 2-6, days 6-10, or days 10-14. Forced expression of Hex could induce *Alb* mRNA only when Dox was added between days 6-10, but not when added earlier (days 2-6) or later (days 10-14) than these times (Fig. 3A). Next, Dox was added to the EB cultures for a 24-hour period between days 5 and 9 of differentiation. *Alb* expression was measured at day 14 of culture using real-time PCR. As shown in Fig. 3A, *Alb* message was only increased in the population in which *Hex* was induced at day 6 for 24 hours. Induction at earlier or later time points had little effect on *Alb* expression. These findings suggest that *Hex* expression during this narrow stage of differentiation is critical for hepatic specification of the ESC-derived endoderm.

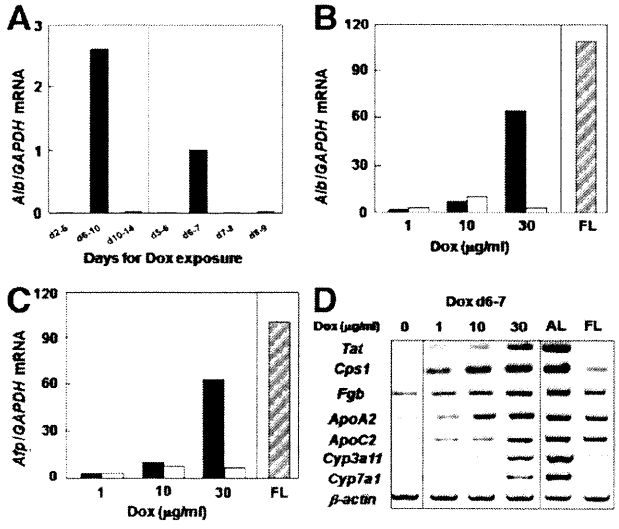

Fig. 3. Dox induction of hepatocyte differentiation is stage-specific and concentration-dependent. (A) Dox was applied at the indicated time points and duration and *Alb* mRNA levels were measured on day 14. (B,C) Dox was added at the indicated concentrations on days 6-7 (black bars) or from day 6 to day 10 (white bars). Levels of *Alb* (B) and *Afp* (C) mRNA were measured on day 14. *Alb* and *Afp* mRNA levels were quantified by way of real-time PCR and normalized to *GAPDH* mRNA levels. *Alb* and *Afp* mRNA levels are indicated as the ratio compared with those in day 14 fetal liver (A-C). FL, day 14 fetal liver. (D) RT-PCR analysis of genes associated with liver maturation. Dox was added at indicated concentrations on days 6-7 and expression patterns were analyzed on day 14. AL, adult liver; FL, day 14 fetal liver.

When next evaluated the effects of Dox concentration and the duration of induction on the levels of *Alb* expression. At concentrations of 1 and 10 μg/mL, Dox induced dose-dependent expression of *Alb* (Fig. 3B) and *Afp* (Fig. 3C), regardless of the duration of Dox exposure. Interestingly, exposure to a higher concentration of Dox (30 μg/mL) for 1 day increased *Alb* and *Afp* expression dramatically, to levels of 60% and 62% of those found in day 14 fetal liver (Fig. 3B,C). With the high concentrations of Dox, however, we observed a significant decrease in size (up to 75%) of the resulting EBs. The up-regulated expression of *Alb* and *Afp* by *Hex* was dependent on prior induction of endoderm by activin, as no expression was detected serum-induced EB that contained mesoderm and little, if any endoderm (data not shown). A longer exposure (4 days) to 30 μg/mL of Dox disrupted EB differentiation and suppressed expression of *Alb* and *Afp* mRNA.

In addition to *Alb* and *Afp*, other genes involved in hepatocyte maturation and function, including tyrosine aminotransferase, *Cps1*, fibrinogen β, apolipoprotin A2 (*Apo A2*), *Apo C2*, cytochrome P450 (*Cyp3a11* and *Cyp7a1*) were also induced in the population generated from EBs treated with high concentrations (30 μg/mL) of Dox on day 6 (Fig. 3D). Consistent with the expression data, we observed that secretion of Alb and transferrin increased with increasing concentrations of Dox, reaching levels of 12.6 and 2.9 μg/mg protein/24 hours, respectively, following induction by 30 μg/mL Dox (Fig. 2C,D). These levels of secretion were 84% and 48% of that of day 14 fetal liver cells, respectively.[23]

Hex Induces Hepatocyte-Related Genes in the c-kit$^+$ Endodermal Cells. The above studies indicate that Hex induces a hepatic fate in the context of the whole EB population. We have previously demonstrated that endoderm segregates to the c-kit^{high}/CXCR4$^+$ brachyury-positive (GFP-Bry$^+$) population of activin-induced EBs.[18] The studies of Tada et al.[24] have shown that activin induced endoderm also express E-cadherin (ECD). As shown in Fig. 4A, activin induced a GFP-Bry$^+$/c-kit^{high} population in a dose-dependent fashion over a 6-day period. Analyses of ECD expression indicated that the majority of the c-kit+ population induced with high concentrations of activin also expressed ECD (Fig. 4B). Molecular analyses revealed that the c-kit+ population isolated from day 6 activin-induced EBs expressed genes indicative of endoderm induction, including Foxa2, *Sox17*, *Cereberus*, and those associated with hepatic (*Hex*) and pancreatic (*Ipf1*) specification (Fig. 4C). Immunocytochemical analysis showed that the incidence of Foxa2$^+$ cells within the c-kit^{high} population was much higher than within the GFP-Bry$^+$/c-kit^{low} population (Fig. 4D). Together, these analyses confirm that the c-kit^{high} population is enriched for endoderm. We next sorted the GFP-Bry$^+$/c-kit^{high} and GFP-Bry$^+$/c-kit^{low} fractions from day 6 activin-induced EBs and cultured the cells at high density in the presence of Dox (1 μg/mL) for 4 days. Under these conditions the cells will reaggregate and form EB-like structures that support the continued differentiation of the respective populations. *Alb* message was only induced in the endoderm-enriched c-kit^{high} population, clearly demonstrating that Hex functioned to specify a hepatic fate directly in definitive endoderm (Fig. 4E).

Hex and BMP-4 Act in Concert to Induce Alb Expression During EB Differentiation. We have previously demonstrated that BMP-4 signaling induces a hepatocyte fate in activin-induced endoderm during EB differentiation.[18] To further examine the relationship between BMP-4 and Hex, day 6 activin-induced EBs were exposed to BMP-4, to Dox (1 μg/mL) or to both BMP-4 and Dox (1 μg/mL) from days 6 to 10. As previously shown, BMP-4 did induce *Alb* and *Afp* mRNA (Fig. 5A). The levels of *Alb* and *Afp* mRNA detected in day 14 hepatocyte cultures reached 19.7% and 25.8% of those found in day 14 fetal liver, respectively, and were much higher than those induced by 1 μg/mL of Dox (days 6-10). The addition of basic fibro-

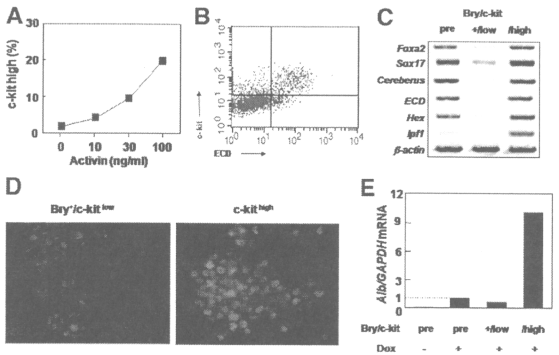

Fig. 4. Endoderm potential of c-kit^{high} cells and *Hex*-induced hepatocyte differentiation in activin-induced endoderm. Tet-Hex Bry-Ainv cells were cultured for 2 days in SP34, after which EBs were transferred to SR medium containing various concentrations of activin. (A) Dose-dependent induction of c-kit^{high} cells on day 6. (B) Fluorescence-activated cell sorting profile for c-kit and ECD in day 6 EBs stimulated by activin (100 ng/mL). (C) RT-PCR analyses of endoderm-related genes in the presorted (pre), GFP-Bry+ c-kit^{low}, and GFP-Bry+c-kit^{high} day 6 EB populations. (D) Immunostaining of Foxa2 in GFP-Bry$^+$/c-kit^{low} GFP-Bry$^+$/c-kit^{high} cells from day 6 activin-induced EBs. (E) Expression of *Alb* mRNA in EBs on day 14 from the different day 6 EB-derived populations. Cells from the pre-sorted or sorted populations were reaggregated with or without Dox (1 μg/mL) from day 6 to 10, cultured in SR medium, and replated on day 10. Levels of *Alb* mRNA normalized to those of *GAPDH* mRNA in day 14 EBs are shown. *Alb* mRNA levels were indicated as the ratio compared with those in day 14 fetal liver.

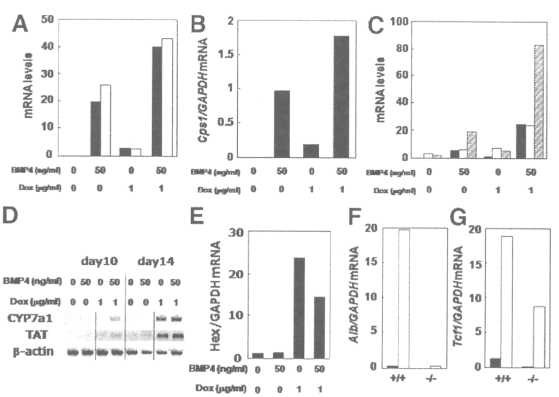

Fig. 5. BMP-4 and Hex act synergistically to enhance expression of liver-related genes during EB differentiation. (A-E) Tet-Hex ESCs induced by activin between day 2 and day 6 of differentiation were stimulated with BMP-4 (50 ng/mL) and/or *Hex* (Dox; 1 μg/mL, days 6-10) as indicated. (A) Expression of *Alb* (black bars), *Afp* (white bars), and (B) *Cps1* were evaluated on day 14. (C) Expression of *Afp* (black bars), *Cebpa* (white bars), and *Tcf1* (striped bars) were evaluated on day 10. (D) CYP7a1 and TAT were evaluated on day 10 and day 14 by way of RT-PCR. (E) Expression of Hex was evaluated on day 10. (F,G) *Hex*$^{+/+}$ (+/+) or *Hex*$^{-/-}$ (−/−) ESCs were cultured in the absence (black bars) or the presence (white bars) of BMP-4 from day 6 to day 10. Levels of *Alb* (F) and *Tcf1* (G) mRNA were measured on day 14 and day 10, respectively. Gene expression levels were quantified using real-time PCR and normalized to those of *GAPDH* mRNA. Levels of *Alb*, *Afp*, *Tcf1*, and *Cebpa* mRNA were indicated as the ratio compared with those in day 14 fetal liver (A,D,F,G). *Cps1* mRNA levels (B) were indicated as the ratio compared with those in adult liver, because fetal liver does not express this gene.

blast growth factor, hepatocyte growth factor, and vascular endothelial growth factor had no effect on *Alb* and *Afp* expression (data not shown). Interestingly, the combination of BMP-4 and Dox further increased *Alb* and *Afp* mRNA levels to 40.3% and 43.3% of those found in day 14 fetal liver, respectively (Fig. 5A). Expression of *Cps1*, a gene that encodes carbamoyl-phosphate synthetase 1 expressed in mature hepatocytes, was also synergistically induced in the presence of BMP-4 and Dox on day 14 (Fig. 5B).

To gain further insight into the onset of hepatic development in these cultures, we evaluated the expression of *Tcf1* and *Cebpa*, as these transcription factors are known to play a pivotal role in the establishment of the early liver by directly regulating expression of a variety of genes, including albumin, transferrin, and fibrinogen.[25] Both BMP-4 and Dox (Hex) induced the expression of *Tcf1* and *Cebpa* on day 10 of culture. As observed with the previous set of genes, the combination of BMP-4 and Dox resulted in a synergistic induction of expression of both (Fig. 5C), although the effect on *Tcf1* was significantly greater than that observed on *Cebpa*. Taken together, these results suggest that BMP-4 and Hex function in a synergistic fashion to establish the liver fate, as defined by the up-regulation of expression of *Tcf1*, *Cebpa*, *Alb*, and *Afp*.

In contrast to the above set of genes, neither BMP-4 nor Hex alone induced expression of *CYP7a1* or *TAT*, two genes indicative of hepatic maturation, at day 10 of differentiation (Fig. 5D). The combination of BMP-4 signaling and *Hex* expression did result in low levels of *CYP7a1* and *TAT* expression at this time. By day 14, Hex but not BMP-4 induced *CYP7a1* and *TAT* expression. These findings indicate that maintenance of appropriate levels of *Hex* is essential for maturation of the hepatic lineage in culture.

The effect of BMP-4 does not appear to be mediated directly through Hex, because Hex expression was not up-regulated following BMP-4 treatment of activin-induced endoderm (Fig. 5E). Although BMP signaling did not induce Hex, a functional Hex gene is required for establishment of the liver fate, because BMP-4 was unable to induce *Alb* expression in $Hex^{-/-}$ endoderm (Fig. 5F). In contrast, BMP-4 did induce *Tcf1* expression in the absence of Hex, although the levels were not as high as those observed in the wild-type population (Fig. 5G). Findings from these analyses suggest that Hex and BMP-4 can regulate Tcf1 expression independently, but optimal levels of expression require both pathways. We also evaluate if Hex can induce BMP-4 mRNA levels. However, Hex did not affect the gene expression levels of BMP-4 (data not shown).

To determine if BMP-4 and Hex have an impact on the hepatoblast stage of development, we analyzed the different populations for expression of Dlk1. Tanimizu et al.[26] have shown that Dlk1 is expressed on progenitors with hepatoblast potential as fetal liver cells sorted for this marker displayed both hepatocyte and biliary epithelial potential. Dlk1 message was detected in day 10 EBs cultured in the absence of BMP-4 and Dox induction. Addition of BMP-4, but not the induction of Hex, increased the levels of Dlk1 expression. The relatively high levels of Dlk1 observed in the absence of BMP-4 appear to be a result of activin signaling, because substantially lower levels were detected in cells differentiated in the absence of activin. Induction with BMP-4 doubled the expression levels of Dlk1 in either the absence of presence of activin. Finally, neither factor induced significant levels of Dlk1 in the absence of a functional Hex gene.

Discussion

The directed differentiation of ESCs in culture is emerging as a powerful model system for studying mammalian development *in vitro* as well as a renewable source of functional cell types for transplantation for future cell-based therapy and for drug discovery and toxicology testing.[27] Of the different cell populations that can be generated from these pluripotent stem cells, hepatocytes are of particular interest because hepatocyte-based therapy has been considered as a new generation and effective treatment mode for liver diseases[28] and the liver is a primary target organ of drug toxicity.[29] A number of reports have documented the efficient generation of immature hepatocytes from both mouse and human ESCs,[16-18] demonstrating that specification of this lineage can be studied in this model system. The most successful approaches to date have translated developmental biology to the culture dish and recreated the key aspects of the normal hepatic developmental program in the differentiation cultures. Although these studies collectively show that it is possible to generate populations with hepatic characteristics, the cells that do develop in the cultures remain immature. Complimentary approaches to cytokine-induced differentiation for the generation of functional cell populations include gain- and loss-of-function of key regulatory genes. Using a gain-of-function strategy in this study, we have shown that enforced expression of *Hex* at specific developmental step promotes the differentiation of the hepatic lineage from mouse ESCs.

In the mouse embryo, *Hex* is required for establishment of the fetal liver from the liver bud,[13-15] positioning it at the level of lineage progression and maturation rather than at the earliest specification step. The requirement for *Hex* in progression of the hepatic lineage was also ob-

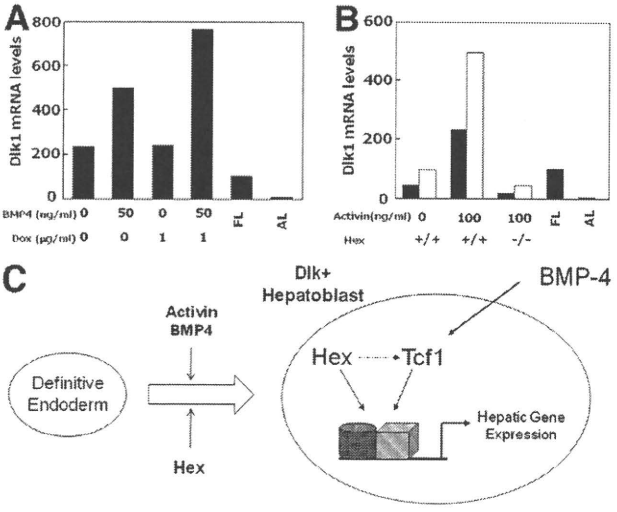

Fig. 6. Regulation of Dlk1 expression by activin, Hex, and BMP-4. (A) Expression of Dlk1 in populations induced with BMP-4, Hex, or both. Tet-Hex ESCs induced by activin between day 2 and day 6 of differentiation were stimulated with BMP-4 (50 ng/mL) and/or *Hex* (Dox; 1 μg/mL, days 6-10) as indicated. Expression of *Dlk1* was evaluated on day 10. (B) Effect of activin and BMP-4 on Dlk1 expression in wild-type (+/+) and Hex null (−/−) ESCs. $Hex^{+/+}$ (+/+) or $Hex^{-/-}$ (−/−) ESCs were cultured in the absence (0 ng/mL) or presence (100 ng/mL) of activin from day 2 to day 6. They were subsequently cultured in the absence (black bars) or presence (white bars) of BMP-4 from day 6 to day 10. Levels of *Dlk1* mRNA were measured on day 10. Gene expression levels were quantified using real-time PCR and normalized to those of *GAPDH* mRNA. AL, adult liver; FL, day 14 fetal liver. (C) Model depicting the role of BMP-4 and Hex in the specification and maturation of the hepatic lineage from ESCs.

served in the ESC differentiation cultures, as the $Hex^{-/-}$ ESC-derived endoderm population expressed significantly lower levels of *Alb* compared to wild-type cells. This observation adds to the growing body of evidence indicating that lineage specification in the *in vitro* differentiation model recapitulates that observed in the early embryo.[30] In contrast to the loss of function, enforced expression of *Hex* dramatically enhanced hepatic differentiation, suggesting that this gene plays a pivotal regulatory role in the progression of the hepatic lineage in culture. The effects of *Hex* expression are striking, because the induced population expressed genes indicative of hepatic maturation (CYP7A1 and TAT) and secreted levels of Alb and transferrin comparable to those secreted by primary rat hepatocytes in culture. These findings highlight the importance of maintaining appropriate levels of Hex expression in promoting maturation of the hepatic lineage in ESC differentiation cultures. Enforced expression of key transcription factors to promote differentiation from ESCs is not a new approach, because it has been effectively used to generate skeletal myocytes[31] and hematopoietic cells with stem cell characteristics.[21] All three studies used the same inducible system, enabling the regulated expression of the gene of interest. While gain-of-function strategies may not be appropriate for the generation of functional cell types for clinical use, the findings from such studies do provide important insights into the key transcriptional pathways that regulate lineage development.

Studies performed initially in the mouse embryo[6] and subsequently in the ESC model[18] have shown that BMP-4 is required for hepatic specification of definitive endoderm. Although the precise relationship of BMP-4 and Hex are not known, the findings from our study are consistent with a model in which both BMP-4 and Hex are required for specification of the hepatoblast from activin-induced definitive endoderm (Fig. 6C). Once the hepatoblast is specified, these factors appear to regulate independent sets of genes that interact at some point to promote hepatic differentiation as suggested by the following observations. First, BMP-4 signaling does not induce Hex expression, indicating that the BMP pathway does not directly regulate this transcription factor. Second, enforced expression of Hex and BMP-4 display synergistic effects in the up-regulation of *Alb* and *Afp* expression. Third, BMP-4 can induce *HNF1/Tcf1*, a key regulator of *Ttr*, *Alb*, *Afp*, fibrinogen α, fibrinogen β, and *ApoA2* expression in the absence of Hex. HNF1/Tcf1 may represent one point of convergence within this regulatory network as the levels of expression induced by BMP-4 are higher in wild-type cells than in the $Hex^{-/-}$ endoderm and dramatically enhanced by the enforced expression of *Hex*. In addition to playing a regulatory role at the level of Tcf1 expression, evidence exists that Hex can physically interact with Tcf1[32] suggesting that these transcription factors may function as coactivators of downstream targets.

In conclusion, the findings presented here document a pivotal role for Hex in the establishment of the hepatic lineage in ESC cultures and in doing so provide further evidence that lineage commitment in this model accurately reflects that observed in the early embryo. Stage-specific enforced expression of Hex promoted hepatic development and maturation, indicating that this strategy may provide an efficient method for the production of relatively mature cell types for studies on lineage commitment, for transplantation in preclinical model of liver disease and for drug discovery and analyses.

Acknowledgment: We thank Mako Yabunouchi and Fumie Otsuka for their excellent technical assistance.

References

1. Wells JM, Melton DA. Vertebrate endoderm development. Annu Rev Cell Dev Biol 1999;15:393-410.

2. Zaret KS. Liver specification and early morphogenesis. Mech Dev 2000; 92:83-88.
3. Duncan SA. Mechanisms controlling early development of the liver. Mech Dev 2003;120:19-33.
4. LeDouarin NM. An experimental analysis of liver development. Med Biol 1975;53:427-455.
5. Jung J, Zheng M, Goldfarb M, Zaret KS. Initiation of mammalian liver development from endoderm by fibroblast growth factors. Science 1999; 284:1998-2003.
6. Rossi JM, Dunn NR, Hogan BL, Zaret KS. Distinct mesodermal signals, including BMPs from the septum transversum mesenchyme, are required in combination for hepatogenesis from the endoderm. Genes Dev 2001; 15:1998-2009.
7. Hromas R, Radich J, Collins S. PCR cloning of an orphan homeobox gene (PRH) preferentially expressed in myeloid and liver cells. Biochem Biophys Res Commun 1993;195:976-983.
8. Crompton MR, Bartlett TJ, MacGregor AD, Manfioletti G, Buratti E, Giancotti V, et al. Identification of a novel vertebrate homeobox gene expressed in haematopoietic cells. Nucleic Acids Res 1992;20:5661-5667.
9. Bedford FK, Ashworth A, Enver T, Wiedemann LM. HEX; a novel homeobox gene expressed during haematopoiesis and conserved between mouse and human. Nucleic Acids Res 1993;21:1245-1249.
10. Thomas PQ, Brown A, Beddington RSP. Hex: a homeobox gene revealing peri-implantation asymmetry in the mouse embryo and early transient marker of endothelial cell precursors. Development 1998;125:85-94.
11. Keng VW, Fujimori KE, Myint Z, Tamamaki N, Nojyo Y, Noguchi T. Expression of Hex mRNA in early murine postimplantation embryo development. FEBS Lett 1998;426:183-186.
12. Bogue CW, Ganea GR, Sturm E, Ianucci R, Jacobs HC. Hex expression suggests a role in the development and function of organs derived from foregut endoderm. Dev Dyn 2000;219:84-89.
13. Keng VW, Yagi H, Ikawa M, Nagano T, Myint Z, Yamada K, et al. Homeobox gene Hex is essential for onset of mouse embryonic liver development and differentiation of monocyte lineage. Biochem Biophys Res Commun 2000;276:1155-1161.
14. Bort R, Martinez-Barbera JP, Beddington RS, Zaret KS. Hex homeobox gene-dependent tissue positioning is required for organogenesis of the ventral pancreas. Development 2004;131:797-806.
15. Barbera JPM, Clements M, Thomas P, Rodriguez T, Meloy D, Kioussis D, et al. The homeobox gene Hex is required in definitive endoderm tissues for normal forebrain, liver and thyroid formation. Development 2000; 127:2433-2445.
16. Chinzei R, Tanaka Y, Shimizu-Saito K, Hara Y, Kakinuma S, Watanabe M, et al. Embryoid-body cells derived from a mouse embryonic stem cell line show differentiation into functional hepatocytes. HEPATOLOGY 2002; 36:22-29.
17. Jones EA, Tosh D, Wilson DI, Lindsay S, Forrester LM. Hepatic differentiation of murine embryonic stem cells. Exp Cell Res 2002;272:15-22.
18. Gouon-Evans V, Boussemart L, Gadue P, Nierhoff D, Koehler CI, Kubo A, et al. BMP-4 is required for hepatic specification of mouse embryonic stem cell-derived definitive endoderm. Nat Biotechnol 2006;24:1402-1411.
19. Fehling HJ, Lacaud G, Kubo A, Kennedy M, Robertson S, Keller G, et al. Tracking mesoderm induction and its specification to the hemangioblast during embryonic stem cell differentiation. Development 2003;130:4217-4227.
20. Kubo A, Chen V, Kennedy M, Zahradka E, Daley GQ, Keller G. The homeobox gene HEX regulates proliferation and differentiation of hemangioblasts and endothelial cells during ES cell differentiation. Blood 2005; 105:4590-4597.
21. Kyba M, Perlingeiro RCR, Daley GQ. HoxB4 confers definitive lymphoid-myeloid engraftment potential on embryonic stem cell and yolk sac hematopoietic progenitors. Cell 2002;109:29-37.
22. Kubo A, Shinozaki K, Shannon JM, Kouskoff V, Kennedy M, Woo S, et al. Development of definitive endoderm from embryonic stem cells in culture. Development 2004;131:1651-1662.
23. Yeoh GC, Wassenburg JA, Edkins E, Oliver IT. Synthesis and secretion of albumin and transferrin by foetal rat hepatocyte cultures. Biochim Biophys Acta 1979;565:347-355.
24. Tada S, Era T, Furusawa C, Sakurai H, Nishikawa S, Kinoshita M, et al. Characterization of mesendoderm: a diverging point of the definitive endoderm and mesoderm in embryonic stem cell differentiation culture. Development 2005;132:4363-4374.
25. Cereghini S, Blumenfeld M, Yaniv M. A liver-specific factor essential for albumin transcription differs between differentiated and dedifferentiated rat hepatoma cells. Genes Dev 1988;2:957-974.
26. Tanimizu N, Nishikawa M, Saito H, Tsujimura T, Miyajima A. Isolation of hepatoblasts based on the expression of Dlk/Pref-1. J Cell Sci 2003;116: 1775-1786.
27. Murry CE, Keller G. Differentiation of embryonic stem cells to clinically relevant populations: lessons from embryonic development. Cell 2008; 132:661-680.
28. Muraca M, Gerunda G, Neri D, Vilei MT, Granato A, Feltracco P, et al. Hepatocyte transplantation as a treatment for glycogen storage disease type 1a. Lancet 2002;359:317-318.
29. Lee WM. Drug-induced hepatotoxicity. N Engl J Med 2003;349:474-485.
30. Keller G. Embryonic stem cell differentiation: emergence of a new era in biology and medicine. Genes Dev 2005;19:1129-1155.
31. Darabi R, Gehlbach K, Bachoo RM, Kamath S, Osawa M, Kamm KE, et al. Functional skeletal muscle regeneration from differentiating embryonic stem cells. Nat Med 2008;14:134-143.
32. Tanaka H, Yamamoto T, Ban T, Satoh S, Tanaka T, Shimoda M, et al. Hex stimulates the hepatocyte nuclear factor 1alpha-mediated activation of transcription. Arch Biochem Biophys 2005;442:117-124.

Fractalkine expression and CD16^{+} monocyte accumulation in glomerular lesions: association with their severity and diversity in lupus models

Kimihiko Nakatani, Shuhei Yoshimoto, Masayuki Iwano, Osamu Asai, Ken-ichi Samejima, Hirokazu Sakan, Miho Terada, Hitoshi Hasegawa, Masato Nose and Yoshihiko Saito

Am J Physiol Renal Physiol 299:F207-F216, 2010. First published 21 April 2010;
doi:10.1152/ajprenal.00482.2009

You might find this additional info useful...

This article cites 26 articles, 9 of which can be accessed free at:
http://ajprenal.physiology.org/content/299/1/F207.full.html#ref-list-1

This article has been cited by 1 other HighWire hosted articles
Fractalkine/CX3CL1: A Potential New Target for Inflammatory Diseases
Brian A. Jones, Maria Beamer and Salahuddin Ahmed
Mol Interv, October, 2010; 10 (5): 263-270.
[Full Text] [PDF]

Updated information and services including high resolution figures, can be found at:
http://ajprenal.physiology.org/content/299/1/F207.full.html

Additional material and information about ***AJP - Renal Physiology*** can be found at:
http://www.the-aps.org/publications/ajprenal

This infomation is current as of January 14, 2011.

AJP - Renal Physiology publishes original manuscripts on a broad range of subjects relating to the kidney, urinary tract, and their respective cells and vasculature, as well as to the control of body fluid volume and composition. It is published 12 times a year (monthly) by the American Physiological Society, 9650 Rockville Pike, Bethesda MD 20814-3991. Copyright © 2010 by the American Physiological Society. ISSN: 0363-6127, ESSN: 1522-1466. Visit our website at http://www.the-aps.org/.

Downloaded from ajprenal.physiology.org on January 14, 2011

Am J Physiol Renal Physiol 299: F207–F216, 2010.
First published April 21, 2010; doi:10.1152/ajprenal.00482.2009.

Fractalkine expression and CD16$^+$ monocyte accumulation in glomerular lesions: association with their severity and diversity in lupus models

Kimihiko Nakatani,[1] Shuhei Yoshimoto,[1] Masayuki Iwano,[1] Osamu Asai,[1] Ken-ichi Samejima,[1] Hirokazu Sakan,[1] Miho Terada,[2] Hitoshi Hasegawa,[3] Masato Nose,[2] and Yoshihiko Saito[1]

[1]*First Department of Internal Medicine, Nara Medical University, Kashihara, Nara; and* [2]*Division of Pathogenomics, Department of Pathology, and* [3]*Department of Bioregulatory Medicine, Ehime University Graduate School of Medicine, Toon, Ehime, Japan*

Submitted 19 August 2009; accepted in final form 15 April 2010

Nakatani K, Yoshimoto S, Iwano M, Asai O, Samejima K, Sakan H, Terada M, Hasegawa H, Nose M, Saito Y. Fractalkine expression and CD16$^+$ monocyte accumulation in glomerular lesions: association with their severity and diversity in lupus models. *Am J Physiol Renal Physiol* 299: F207–F216, 2010. First published April 21, 2010; doi:10.1152/ajprenal.00482.2009.—Fractalkine (Fkn) is expressed on injured endothelial cells and is a membrane-bound chemokine that attracts cells expressing its receptor, CX3CR1, including CD16$^+$ monocytes (CD16$^+$ Mos). To clarify the role played by Fkn in the development of glomerular lesions in lupus nephritis, we examined Fkn expression and CD16$^+$ Mo accumulation induced in experimental C.B-17/Inc-scid/scid (SCID) lupus model mice by injection of IgG_3-producing hybridoma clones obtained from MRL/lpr mice. Glomerular Fkn expression and accumulation of CD16$^+$ Mos were semiquantitatively evaluated using laser capture microdissection and real-time PCR. Injection of the 2B11.3 and 7B6.8 clones induced formation of glomerular proliferative and wire-loop lesions, respectively. Immunohistological analysis of the localization of Fkn and CD16$^+$ Mos revealed that Fkn expression and CD16$^+$ Mo accumulation were markedly elevated in glomerular lesions induced by 2B11.3, whereas no elevation was detected in those induced by 7B6.8. In addition, to examine the contribution of glomerular Fkn to the development of proliferative lesions, L cells producing an Fkn antagonist (Fkn-AT) were transplanted into SCID mice exhibiting proliferative lupus nephritis (DPLN) induced by 2B11.3. Notably, transplantation of the Fkn-AT-producing cells was functionally and histologically protective against this DPLN. Taken together, our findings suggest that Fkn and CD16$^+$ Mo accumulation are partially associated with the severity and diversity of histology of lupus nephritis.

lupus nephritis; fractalkine; CD16$^+$ monocyte; MRL mice; histopathology

SYSTEMIC LUPUS ERYTHEMATOSUS (SLE) is an autoimmune disease in which the deposition of immune complexes (ICs) and autoantibodies leads to the activation of complement systems and subsequent inflammation (17). IC-induced glomerulonephritis in SLE is termed lupus nephritis and is a common complication in SLE (5). Similarly, MRL/lpr mice spontaneously develop a lethal glomerulonephritis with an increase in circulating ICs, autoantibody production, and cytokine abnormalities (3, 20). The glomerular lesions seen in MRL/lpr mice consist of diffuse cell proliferative and/or wire-loop-like lesions that resemble the various histological patterns observed in human lupus nephritis (3, 20). These lesions are characterized by the deposition of ICs and are associated with increases in serum levels of rheumatoid factors and anti-DNA and anti-glycoprotein 70 autoantibodies, which are thought to play major roles in the histopathogenesis of lupus nephritis (6, 16, 22).

The membrane-spanning protein fractalkine (Fkn) is a member of the CX3C family of chemokines and contains a conserved CX3C domain atop a mucin-like stalk in its extracellular region (4). Fkn is expressed at very low levels by resting endothelial cells but undergoes marked upregulation following stimulation of the cells by cytokines such as tumor necrosis factor-α (TNF-α) and interleukin-1β (IL-1β) (4). Fkn is also known to function as a cellular adhesion molecule and to attract cells expressing its receptor, CX3CR1 (4, 12). The Fkn-CX3CR1 interaction has been implicated in the pathogenesis of several renal diseases, including lupus nephritis, acting through the accumulation and/or activation of CX3CR1-positive cells. For instance, proinflammatory CD16-positive monocytes (CD16$^+$ Mos) express CX3CR1 and appear to be preferentially recruited to vessel walls through the chemoattractant property of Fkn (1, 2). Moreover, we previously showed that the expression of Fkn and accumulation of CD16$^+$ Mos within glomeruli are enhanced in human proliferative lupus nephritis, suggesting the interaction between CD16$^+$ Mos and Fkn-expressing cells, and plays an important role in the pathogenesis of human lupus nephritis (26).

We also previously found that IgG_3 production plays a critical role in the development of glomerulonephritis in MRL/lpr mice (25), which prompted us to develop two nephritogenic IgG_3-producing hybridoma clones, 7B6.8 and 2B11.3, from unmanipulated MRL/lpr mice. These clones respectively induce two different types of glomerular lesions when injected in C.B-17/Inc-scid/scid (SCID) lupus model mice: a wire-loop-like lesion and an endocapillary proliferative lesion (14). In the present study, we investigated the levels of Fkn expression and CD16$^+$ Mos accumulation in glomerular lesions induced by clones 2B11.3 and 7B6.8 to assess the role played by Fkn in the generation of glomerular lesions in lupus nephritis. We also established a system for producing an Fkn antagonist (Fkn-AT) in vivo by transplanting L cells expressing the antagonist in mice. We then used this system to evaluate the contribution made by Fkn to the development of lupus nephritis in vivo.

MATERIALS AND METHODS

Mice. MRL/lpr and MRL/Mp$^{+/+}$ (MRL/+) mice were originally purchased from The Jackson Laboratory (Bar Harbor, ME); C.B-17/Inc-scid/scid (SCID) mice were from Japan Clea (Tokyo, Japan). All mice were housed under conditions free of specific pathogens in the Animal Research Institute of Nara Medical University. All procedures involving mice were carried out in accordance with the National

Address for reprint requests and other correspondence: K. Nakatani, First Dept. of Internal Medicine, Nara Medical Univ., 840, Shijo-cho, Kashihara, Nara, 634-8522, Japan (e-mail: nkimihik@ naramed-u.ac.jp).

0363-6127/10 Copyright © 2010 the American Physiological Society

Downloaded from ajprenal.physiology.org on January 14, 2011

Institutes of Health guidelines for the care use of live animals and were approved by the Nara Medical University Animal Care Committees.

Hybridoma clones. IgG_3 antibody-producing hybridoma clones, 2B11.3, 7B6.8, and 1G3, derived from an unmanipulated MRL/lpr mouse were used in this study (14). When injected in SCID mice, the 2B11.3 and 7B6.8 clones induce the endocapillary proliferative and wire-loop types of glomerular lesions, respectively. The 1G3 clone does not induce any glomerular injury (14).

Injections of hybridomas. Hybridoma clones (1×10^7 cells) were intraperitoneally injected in SCID mice. In our earlier study, SCID mice injected with either the 2B11.3 or 7B6.8 clone developed significant glomerular lesions after 15–25 days (21). In the present study, therefore, serum samples and kidneys were collected from mice under ether anesthesia 15–25 days after the injection. We also killed mice under ether anesthesia 10–15 days after the injection to collect serum samples and kidneys at a predisease stage characterized by the deposition of IgG_3 along the glomerular capillary walls without development of histopathological glomerular lesions.

Histopathological and immunohistochemical examinations. For histopathology, tissue samples were fixed with 10% formalin in 0.01 mol/l phosphate buffer (pH 7.2) and embedded in paraffin. They were then stained with hematoxylin and eosin (H&E) or periodic acid-Schiff for examination under a light microscope. The glomerular lesions in SCID mice injected with 2B11.3 clones were graded from zero to three, based on the severity of the glomerular cell proliferation and inflammatory cells infiltration; *grade 0*, normal; *grade 1*, mild; *grade 2*, moderate; and *grade 3*, severe. Index of glomerular lesions means the average grading of 20–30 glomeruli. For immunostaining, pieces of kidney were frozen in 22-oxacalcitriol compound (Miles, Elkhart, IN), after which frozen sections were cut and fixed with cold acetone, and endogenous peroxidase was blocked by incubating the tissue sections in 3% hydrogen peroxide for 15 min. Thereafter, the tissue sections were incubated with biotin-labeled goat anti-murine Fkn polyclonal antibody (R&D Systems, Minneapolis, MN) for 2 h at room temperature, and Fkn expression was detected using an avidin-biotin-peroxidase system (LSAB+ kit; Dako, Carpentaria, CA). Preimmune biotin-labeled goat serum served as a negative control. The phenotype of the infiltrating cells was also analyzed in frozen sections using the avidin-biotin-peroxidase method with a rat anti-mouse CD16 monoclonal antibody (Pharmingen, San Diego, CA). For staining IgG_3, fluorescein isothiocyanate-conjugated rabbit anti-mouse IgG_3 antibodies (ICN ImmnoBiologicals, Lisle, IL) were used.

Tissue preparation and laser-capture microdissection. Frozen kidneys were cut transversely into 7- to 10-μm sections using a cryostat, mounted on uncoated glass slides, and stored at −80°C until use. Tissue dehydration and staining were then accomplished using Histogene laser-capture microdissection (LCM) frozen-section staining reagents as instructed by the manufacturer (Arcturus Engineering, Mountain View, CA) (19, 24). Briefly, sections were fixed and sequentially dehydrated in 75, 95, and 100% ethanol followed by 100% xylene. The sections were then air-dried and stored in a desiccator at room temperature until used for LCM; care was taken to ensure that LCM was completed within 1 h after the slides were placed in the desiccator. Two or three sections from each sample were stained with H&E to verify the quality of the sections. LCM was then carried out using a PixCell II LCM System (Acturus Engineering). Targeted glomeruli were selectively captured from each section, and a total of 50–100 glomeruli were obtained from each specimen (typically from 6–8 slides). Targeted glomeruli contained lesions characterized by *1*) pure mesangial proliferation in 4-wk-old MRL/lpr mice (Fig. 1*A*); *2*) endocapillary proliferation with inflammatory cell infiltration and segmental wire-loop-like lesions in 20-wk-old MRL/lpr mice (Fig. 1*B*); *3*) pure endocapillary proliferation with inflammatory cell infiltration in SCID mice injected with the 2B11.3 clone (see Fig. 3*A*); *4*) little inflammatory cell infiltration, despite IgG_3 deposition in mesangial areas and along the capillary walls in SCID mice injected with 2B11.3 clone at the predisease stage (see Fig. 5*A*); and *5*) hyaline deposits along capillary walls and thrombi composed in part of hyaline within capillaries of SCID mice injected with 7B6.8 clone (see Fig. 3*B*).

RNA isolation and real-time PCR assay. Total RNA preparations were produced from 50–100 glomeruli obtained using LCM with a Pico pure RNA isolation kit (Arcturus Engineering) (19). Total RNA was extracted from the captured cells by incubating the LCM caps in extraction buffer for 30 min at 42°C, after which the RNA was purified using preconditioned MiraCol (Arcturus Engineering) purification columns. Total RNA was also extracted from primary cultured cells using TRIzol reagent (Life Technologies, Rockville, MD) according to the manufacturer's procedure. First-strand cDNA was then made from the total RNA using a SuperScript Preamplification System (Invitrogen, Carlsbad, CA) with random hexamers. For real-time PCR, 1 μl of each first-strand reaction product was amplified using appropriate primers and corresponding fluorescent probes designed by the Applied Biosystems "Assay-on-Demand" service for mouse and human Fkn (assay ID: Mn00436454_ml, Hs00171086_ml) and mouse and human β-actin (assay ID: Mn01205647_gl, Hs03023943_gl). Fkn-to-β-actin mRNA ratios were calculated for each sample.

Culture of human umbilical vein endothelial cells and primary murine mesangial cells with TNF-α and IL-1β. Human umbilical vein endothelial cells (HUVECs) and their culture medium were from Clonetics (Walkersville, MD). The cells were grown at 37°C on gelatin (Sigma Chemical)-coated flasks (Costar, New York, NY). Primary cultures of murine mesangial cells (MCs) were obtained from outgrowths of isolated mouse renal glomeruli, as described previously (15). The cells were grown at 37°C on plastic petri dishes (Nunc, Roskilde, Denmark) in RPMI 1640 medium containing 20% FCS. Once the cells were semiconfluent, they were passaged after trypsinization. HUVECs and MCs at passages 3–8 were grown to confluence in six-well culture plates and then incubated for 6 h in fresh serum-free RPMI containing TNF-α (Wako Pure Chemical Industries, Osaka, Japan) and IL-1β (Wako Pure Chemical Industries), as indicated in the individual experiments.

Construction of expression vectors encoding murine NH_2-terminal truncated Fkn (Fkn-AT). We used the following specific primers for murine Fkn (23) to amplify fragments containing functional Fkn coding regions (Fkn analog): 5′-ACTCCAGCCATGGCTCCCTCG-3′ (forward) and 5′-CTCACTTGCCACCATTTTTAGTGAG-3′ (reverse). The reverse primer contained the stop codon. Total cellular RNAs were extracted from murine spleen cells, with or without phytohemagglutinin stimulation, as described previously (10). The aforementioned fragments were then amplified by RT-PCR using an RNA PCR kit (Takara Shuzo, Kyoto, Japan) as described previously (10). Forward primers for an NH_2-terminal truncated Fkn analog were prepared using 21-base oligonucleotide sequences corresponding to a truncated Fkn analog in which four amino acid residues were removed from the NH_2-terminus (Fkn-AT). To convert the truncated analogs into their secretory forms, a 67-bp oligonucleotide containing the signal sequence from human interferon-β (18) (5′-CATGACCAACAAGTGTCTCCTCCAAATTGCTCTCCTGTTGTGCTTCTCCACTACAGCTCTTTCCATG-3′) was added to the beginning of each forward primer. The amplified fragments were also cloned into the *Eco* RI site of the pCXN2 vector.

Cell transfection and selection of Fkn-AT transfectants. Mouse L cells [mouse fibroblastic cells (L292) at passages 10–15, purchased from the ATCC] were transfected with 10 μg of pCXN2 vector carrying the Fkn truncated analog gene (Fkn-AT) using Lipofectamine (Life Technologies) as described previously (11). Clones showing the strongest expression of this gene were then selected for further study. Mouse L cells were also transfected with 10 μg of an empty pCXN2 vector, as a control.

Chemotaxis assay. Chemotaxis by murine spleen cells was assayed in Transwell culture chambers with polycarbonate membranes (6.5-mm diameter, 5-μm pore size) (Costar, Cambridge, MA), as

Downloaded from ajprenal.physiology.org on January 14, 2011